

This item is the archived peer-reviewed author-version of:

Nonlinear vibration response measured at umbo and stapes in the rabbit middle ear

Reference:

Peacock John, Pintelon Rik, Dirckx Joris.- Nonlinear vibration response measured at umbo and stapes in the rabbit middle ear

Jaro: journal of the Association for Research in Otolaryngology / Association for Research in Otolaryngology [Mount Royal, N.J.] - ISSN 1525-3961 - 16:5(2015), p. 569-580

Full text (Publishers DOI): <http://dx.doi.org/doi:10.1007/s10162-015-0535-7>

To cite this reference: <http://hdl.handle.net/10067/1287000151162165141>

1 **Abstract**

2 Using laser vibrometry and a stimulation and signal analysis method based on multisines,
3 we have measured the response and the nonlinearities in the vibration of the rabbit middle
4 ear at the level of the umbo and the stapes. With our method we were able to detect and
5 quantify nonlinearities starting at sound pressure levels of 93 dB SPL. Further research will
6 be needed to pinpoint the source of these nonlinearities, but the current results show that no
7 significant additional nonlinearity is generated as the vibration signal is passed on through
8 the middle ear chain.

9 Nonlinearities are most prominent in the lower frequencies (125 Hz to 1 kHz), where their
10 level is about 40 dB below the vibration response at an input of 120 dB SPL. The level of
11 nonlinearities rises with a factor of nearly 2 as a function of sound pressure level, indicating
12 that nonlinear distortions may become important at very high sound pressure levels, such as
13 are used in high-power hearing aids.

14

15 **1. Introduction**

16 Nonlinearity in the mammalian middle ear has been investigated by several authors and
17 using a variety of techniques. The purpose of most of these studies was to exclude the
18 influence of middle ear nonlinearity on other measurements. One of the earliest attempts to
19 measure nonlinearity was made by Guinan and Peake (1967). They measured the motion of
20 the stapes in cats and reported that it behaves linearly up to around 130 dB SPL for
21 frequencies below 1500 Hz, and 140 to 150 dB SPL for higher frequencies. More than a
22 decade later, Nedzelnitsky (1980) measured intracochlear pressures in cats and found them
23 to be linearly related to sound pressure at the eardrum up to 140 dB SPL. Measurements in
24 human temporal bones were performed by Goode et al. (1994). They used laser Doppler
25 vibrometry to measure both the umbo and the stapes and observed no signs of nonlinearity
26 at sound pressure levels below 124 dB. In 2000, Voss et al. also measured stapes velocity
27 and found no signs of nonlinearity below 130 dB SPL. Given these results, the transfer
28 function of the middle ear was assumed to be completely linear up to 130 dB SPL.

29 In 2010 a new, very sensitive method based on multisine excitations was developed and
30 was used to measure the middle ear of gerbils (Aerts and Dirckx, 2010). These new
31 measurements detected small nonlinear distortions appearing above the noise at around 96
32 dB SPL. However, these measurements only examined the vibration response of the umbo,
33 and did not comment on the effects of transmission through the ossicular chain.

34 Everyday sound levels will seldom surpass 100 dB SPL. However, users of high power
35 acoustic hearing aids can be exposed to much higher input pressures, with some modern
36 hearing aids delivering sounds pressure levels as high as 140 dB (such as with the Phonak
37 Naida Q-UP, Phonak, Switzerland). The middle ear then has to transport these very high
38 sound intensities to the inner ear. In such circumstances, the contribution of middle ear
39 nonlinearity may become important. In work on quasi-static pressure response, a strong
40 nonlinear behaviour of both eardrum and stapes displacement has been reported (Dirckx
41 and Decraemer 2001), which suggests that nonlinearities may also become important at
42 high pressure acoustic inputs.

43 The cochlea itself also has strong nonlinear characteristics, resulting in the production of oto-
44 acoustic emissions. These nonlinearities are generated in response to incoming sound
45 which has passed through the middle ear. Therefore better knowledge of nonlinear
46 characteristics of the incoming vibrations opens up the possibility to correctly measure
47 otoacoustic emissions at higher sound pressure levels.

48 It is known that the ossicular chain shows some flexibility (e.g. Willi, Ferrazzini, and Huber,
49 2002, Funnell et al, 2005), and the 3D vibrations of the ossicles become complex at high
50 frequencies (e.g. Hato, Stenfelt, & Goode, 2003). These observations show that the system
51 is not just a simple lever. The individual ossicles themselves may also show some flexibility
52 and change the vibration signal; modelling of the manubrium in cats, for example, has shown
53 it to bend (Funnell, Khanna, and Decraemer, 1992). To quantify the nonlinear vibration input
54 to the cochlea, measurements are therefore not only needed at the level of the umbo but
55 also at the level of the footplate. Such measurements will show if additional nonlinearities
56 are generated as sound is passed through the middle ear.

57 This paper reports measurements of the nonlinearities at the umbo and the footplate in
58 rabbit ears. A very sensitive measurement technique, using multisine excitation signals
59 specially designed for the detection of nonlinearities, was used to quantify the level of
60 nonlinear vibration response at both the umbo and footplate.

61

62 **2. Materials and methods**

63 **2.1 Measurement setup**

64 Measurements were made on five ears removed from four adult male rabbits. The temporal
65 bones were dissected from the skull and a hole was drilled in the bulla to expose the
66 eardrum and allow free visual access perpendicular to the umbo. Next, the cochlea was

67 drilled away to expose the stapes footplate, and allow visual access perpendicular to that.
68 Care was taken during this procedure to ensure that the annular ligament and the bone
69 surrounding the footplate remained intact. The rabbit was chosen over the gerbil as an
70 animal model because the complex preparation procedures have more chance of success in
71 a larger ear.

72 With the middle ear exposed, small pieces (approximately 1 x 1 mm) of reflective tape
73 (Polytec, Germany) were attached to the measurements points. One end of a small plastic
74 tube was glued to the opening of the ear canal, while the other end was attached to an
75 earphone speaker. The tube had a small hole drilled in its side through which the sound
76 pressure level could be measured with a probe microphone (Bruel & Kjaer, type 4182).
77 Throughout the preparation, and between subsequent measurements, the specimen was
78 kept moist using the vapour produced by an ultrasonic humidifier (Bionaire BT-204).

79 The vibrations of the umbo and footplate were measured with a laser vibrometer (Polytec
80 model OFV-534) coupled to a surgical microscope. In this setup the laser spot was
81 positioned using a motor controlled tilting mirror placed in front of the vibrometer. The signals
82 to the speaker were designed in custom built software using Matlab. An A/D–D/A conversion
83 board (RME HDSP 9632) with 24-bit resolution and a sampling rate of up to 192 kHz was
84 used to generate and record the input and output signals.

85 Figure 1A shows a photograph of the rabbit ear as seen through the surgical microscope
86 after preparation. This photograph is of a dried out specimen, taken some time after the
87 measurements. The measurement points are indicated and the small pieces of reflective
88 tape are visible. The direction of the laser beam is perpendicular to the plane of the
89 photograph.

90 Figure 1B shows a snapshot of a 3D image of the rabbit ear based on micro-CT data. The
91 sample was adjusted to try and ensure the laser was measuring at right angles to the
92 footplate and at right angles to the tympanic ring.

93 All experiments were conducted in accordance with all relevant legislation and the directives
94 set by our local ethics committee.

95

96 **2.2 The multisine excitation method**

97 The nonlinear distortions are measured using random phase multisines, which are described
98 mathematically by the following equation:

$$S(t) = \frac{1}{\sqrt{N}} \sum_{k=1}^N A_k \sin(2\pi k f_{res} t + \varphi_k)$$

99 The signal is a multisine consisting of N harmonically related sines (all frequencies being
 100 multiples of f_{res}) with user defined amplitudes (A_k) and random phases (φ_k). The phases are
 101 randomly chosen such that the expected value $\mathbb{E}\{e^{i\varphi_k}\}$ is zero, for example, uniformly
 102 distributed in $[0, 2\pi]$. The excited harmonics are chosen by the user to be within a certain
 103 frequency band from f_{min} to f_{max} . The frequencies are spaced quasi-logarithmically, i.e. the
 104 harmonics are logarithmically spaced but chosen to coincide with the frequency grid
 105 determined by the frequency resolution f_{res} .

106 If a random phase multisine is used as the input to a system, a multisine will be recorded at
 107 the output. Each harmonic in the output signal will consist of a linear contribution from that
 108 harmonic in the input signal, and a nonlinear component from all the other harmonics. If a
 109 random phase multisine containing only odd harmonics is used at the input then only the odd
 110 degree nonlinearities in the system will contribute to the odd harmonics, the even degree
 111 nonlinearities will only contribute to the even, non-excited, harmonics.

112 Thus using only odd random phase multisines allows us to detect the level of even degree
 113 nonlinear distortions by measuring the even harmonics in the output spectrum. In order to
 114 determine the level of the odd degree distortions we need to randomly eliminate some odd
 115 harmonics from our input signal, and measure these at the output.

116 The measurement method proceeds as follows:

117 1. We first choose the measurements time (and thus the frequency resolution f_{res}), the
 118 frequency range (f_{min} and f_{max}), the frequency grid (linear or logarithmic) and the amplitude
 119 spectrum.

120 2. We divide up our odd excited harmonics into groups and randomly eliminate one
 121 harmonic from each group.

122 3. We randomly choose our phases (φ_k) and calculate our excitation signal, $s(t)$. We output
 123 the signal and adjust its amplitude spectrum until we measure the desired stimulus levels.

124 4. We apply the signal to our system and measure P periods of the input ($s_i^P(t)$) and output
 125 ($s_o^P(t)$) signal.

126 From the P noisy output spectra $S_o^P(f)$, one can calculate the mean \hat{S}_o at the excited
 127 harmonics f_{ex} , which gives the output response level, and the standard deviation of the
 128 mean $\sigma_{\hat{S}_o}$, which gives the noise level.

$$\hat{S}_o(f_{ex}) = \frac{1}{P} \sum_{p=1}^P S_o^p(f_{ex})$$

$$\sigma_{\hat{S}_o} = \sqrt{\frac{1}{P(P-1)} \sum_{p=1}^P |S_o^p(f_{ex}) - \hat{S}_o(f_{ex})|^2}$$

129 To get the level of the nonlinear distortions the output spectra $S_o^p(f)$ have to first be
 130 corrected for nonlinear distortions in the input spectra $S_i^p(f)$. Therefore the frequency
 131 response function has to be calculated at the excited harmonics f_{ex} for each measured
 132 period.

$$G^p(f_{ex}) = \frac{S_o^p(f_{ex})}{S_i^p(f_{ex})}$$

133 with $p = 1, \dots, P$.

134 If the test object behaves dominantly linear, a first order correction is obtained by subtracting
 135 the linear contribution of the test object from the output at the non-excited harmonics f_{nex} .

$$S_{oc}^p(f) = \begin{cases} S_o^p(f_{ex}) \\ S_o^p(f_{nex}) - G^p(f_{nex})S_i^p(f_{nex}) \end{cases}$$

136 The frequency response at the non-excited harmonics is obtained by linear interpolation of
 137 the frequency response at the excited harmonics. Using these corrected output spectra, the
 138 level of the nonlinear distortions at the excited harmonics f_{ex} can be calculated by linear
 139 interpolation of the signal at the odd non-excited harmonics.

140 The signal used in the present measurements consisted of quasi logarithmically spaced
 141 frequencies between 125 and 16000 Hz. As explained before, the excited frequencies are
 142 harmonically related so they do not coincide exactly with logarithmically increasing frequency
 143 steps. Instead, harmonically related frequencies are used which are closest to the eight
 144 logarithmically spaced frequencies in each octave.

145 The number of excited harmonics should be large enough so that the middle ear dynamics
 146 are measured with a sufficiently large frequency resolution. Some prior knowledge or
 147 physical insight is typically used to set this number. In this case the prior knowledge was
 148 based on response measurements on a very fine frequency scale, showing smooth
 149 response curves which can be well represented by eight frequencies per octave. On the
 150 other hand the number of excited harmonics should not be too large in order not to
 151 deteriorate the signal-to-noise ratio per excited harmonic. Hence, a trade-off between

152 frequency resolution and signal-to-noise ratio must be made. When using more harmonics,
153 the energy of the nonlinear response will be divided over more frequency lines, so
154 detectability of nonlinearities will decrease. If we use less stimulation frequencies, the total
155 level of the nonlinearities will remain the same, hence in each detection line the signal to
156 noise ratio will be better so the appearance of nonlinearities will be detectable at a lower
157 sound pressure level.

158 In the current study we chose to use eight frequencies per octave as a trade-off between
159 good frequency resolution and good detectability. To optimise this choice a two-step
160 procedure was followed: in a first measurement the signal-to-noise ratio was determined
161 together with the dynamics, this information is then used to determine a good value of the
162 number of excited harmonics in the second experiment. In our measurements we only excite
163 the odd harmonics, the even harmonics are left unexcited for two reasons: (i) in order not to
164 increase the variability of the estimated dynamics, and (ii) to distinguish the even from the
165 odd nonlinear distortions at the output. The odd detection lines are selected by eliminating
166 one randomly selected odd harmonic out of two or three consecutive harmonics. Proceeding
167 in this way the level of the odd nonlinear distortion at the excited odd harmonics is given by
168 the level of the nearest non-excited odd harmonic (Schoukens et al. 2009).

169 Using this method we measured the vibration response, nonlinear distortions, and noise
170 level in five rabbit ears at eleven sound pressure levels ranging from 90 dB SPL to 120 dB
171 SPL in steps of 3 dB.

172

173 **3. Results**

174 The data we recorded is three dimensional: vibration responses and distortion levels are a
175 function of both frequency and sound pressure level. So, we will present two sets of graphs,
176 one set showing data as a function of frequency at different sound pressure levels, the other
177 set showing data as a function of sound pressure level at different frequency octave bands.
178 To give an idea of inter specimen variability we will first show data for all ears at one sound
179 pressure level and in one frequency band. Then we will show averaged data in more detail.

180 At 120dB one of the ears showed anomalous behavior, we suppose some technical problem
181 generated this deviation, but we could not pinpoint its source. So, for all further calculations
182 we used all five ears except for the sound pressure level of 120 dB where we only used 4
183 ears and left out the outlier. In presenting the results from individual ears, we therefore used
184 data measured at 117 dB, so as to show five ears.

185 *Effect of removing the cochlea*

186 In order to be able to measure on the footplate, the cochlea needed to be removed. To
187 examine the effect of this procedure we measured the vibration response and nonlinear
188 distortions at the Umbo before and after drilling open the cochlea. We measured on three
189 separate temporal bones; the results are shown in figure 2.

190 The vibration response of the three bones barely showed any change after removing the
191 cochlea. Only at the resonance peak at around 1800 Hz is a difference noticeable, with the
192 response generally showing less of a peak with the cochlea intact. The nonlinear distortions
193 show slightly more variation, and the nonlinearities appear over most frequencies to be
194 slightly lower than the level with the cochlea intact.

195

196 *Vibration response and nonlinearities in Individual ears*

197 Figure 3A shows the vibration response measured at the umbo for an input sound pressure
198 level of 117 dB. Figure 3B shows the data obtained at the stapes. We see that there is little
199 variability among the different ears, and that the stapes curves resemble the curves obtained
200 at the umbo. Figure 3C shows the ratio of umbo vibration response to stapes vibration
201 response for all five ears: the ratio is nearly constant at about 10dB over the entire frequency
202 range between 125 Hz and 4 kHz, but slightly diminishes at the higher frequencies.

203 Figure 4A shows the level of the nonlinearities measured at the umbo for a sound pressure
204 level of 117 dB. There is more variability between ears than for the vibration response, but
205 the curves are still close to each other. Comparing these curves to the vibration response
206 presented in Figure 3A, we see that the nonlinearities are about 40 dB lower. Comparable
207 results were obtained at all other sound pressure levels. In Figure 4B we see the
208 nonlinearities measured at the stapes: again variability between ears is a bit larger than for
209 the vibration response, but it is still rather limited. Figure 4C then shows the ratio of
210 nonlinearity levels at the umbo and at stapes. All curves are again rather close, but there is
211 of course some more variability between measurement points. On average the ratio is again
212 on the order of 10 dB, just like the ratio of the vibration responses, except at higher
213 frequencies where there appears a slight tendency for the ratio to decrease.

214

215 *Average results*

216 For all following figures, an average was taken over the five measured ears, except at a
217 sound pressure level of 120 dB where only four ears were used. In all plots we have added
218 whiskers to indicate the standard deviation. All calculations were done using dB values.
219 While this is not the same as performing the calculations using linear values, this is
220 commonly done when reporting audiological data and serves to give an impression of the
221 variability in the data.

222 Figure 5 shows the total vibration response (squares) and nonlinear distortions (triangles) as
223 a function of frequency for sound pressure levels of 90 dB (A), 108 dB (B) and 117 dB (C) for
224 the umbo (red) and the stapes (blue). The noise floor is indicated by the dashed line. For
225 frequencies between 125 Hz and 1000 Hz the vibration response curves are rather flat, at
226 1800 - 1900 Hz we see a small resonance peak, and at higher frequencies the response
227 curve becomes a bit more complicated and shows a gradual roll-off. The shape of the
228 response curves of the stapes and umbo are largely identical, and remain practically the
229 same for increasing sound pressure levels. At 90 dB SPL the nonlinearities hardly exceed
230 the noise, but at 120 dB SPL they are clearly visible. The nonlinearity curves obtained for
231 umbo and stapes have a rather good resemblance. Standard deviations on the data points
232 are moderately larger for the nonlinearities than for the vibration response as the level is
233 much lower and the contribution of noise becomes more important.

234 In order to better evaluate differences between umbo and stapes response, figure 6 shows
235 the ratio of umbo to stapes vibration response (red) and nonlinearities (blue) as a function of
236 frequency, measured at 117 dB SPL. The vibration response ratio is fairly flat across the
237 entire frequency range. For frequencies ranging from 125 Hz to about 4 kHz the ratio is
238 between 10.5 dB and 12 dB. At lower sound pressure levels we found similar results, with a
239 slight increase of the ratio to about 13 -16 dB at 90dB SPL.

240 The ratio of the nonlinear distortions shows more variability than the ratio of vibration
241 response. The standard deviations are larger than for the vibration response curve, but for
242 frequencies between 250 Hz and 8 kHz we find a ratio of about 5 to 15 dB. At the lowest
243 measured frequency (125 Hz) the ratio drops to just under 0 dB, but it should be noticed that
244 at such low frequencies the sensitivity of the vibrometer goes down and noise level
245 increases.

246 Figure 7 shows the total vibration response (squares) and nonlinear distortions (triangles) as
247 a function of sound pressure level for the frequency bands 250-500 Hz (A), 1-2 kHz (B) and
248 4-8 kHz (C), for the umbo (red) and the stapes (blue). Error bars again indicate the standard
249 deviation over the individual ears, and the noise floor is indicated by the dashed line. In all
250 figures we see similar behaviours: the response curves of umbo and stapes are practically

251 parallel, the distance between the nonlinearity curves varies a bit more but is also rather
252 constant. In the 1-2 kHz octave the nonlinearity of the umbo response begins to rise above
253 the noise level at 93 dB, and for the stapes it rises above the noise at 99 dB. In the 4-8 kHz
254 octave the Stapes response rises above the noise at 102 dB SPL. In the lowest octave, 250
255 - 500 Hz, the noise floor is somewhat higher, and the nonlinearity in the stapes response
256 becomes visible at 108 dB SPL.

257 In Figure 8 we show the ratio of umbo vibration response to stapes vibration response (red),
258 and the ratio of the nonlinearity of umbo vibration response to stapes vibration response
259 (blue), for the frequency bands 250-500 Hz (A), 1-2 kHz (B) and 4-8 kHz (C). For the
260 nonlinearities, data is only shown when the signals for both umbo and stapes are both above
261 the noise floor. In all three octaves we see that the ratio of umbo vibration response to
262 stapes vibration response is a nearly flat function of sound pressure level. In the 250-500 Hz
263 octave the ratio is 7 dB, while in the 1-2 kHz and 4-8 kHz octaves it has a slightly higher
264 value of around 9 dB. At the very highest sound pressure level of 120 dB SPL we see a
265 small drop in the ratio of about 2 dB in all octaves. The ratio of umbo nonlinearity to stapes
266 nonlinearity is somewhat less constant as a function of sound pressure level, but variations
267 are small. In all octaves we see that the nonlinearity ratio has a slight tendency to increase
268 as a function of sound pressure level, meaning that nonlinearities at the level of the umbo
269 rise slightly faster, as a function of sound pressure level, than nonlinearities at the level of
270 the stapes, but the effect is limited to less than 7 dB in all octaves.

271 In Figure 9 we finally try to give a three dimensional representation of our results. The figure
272 shows the ratio of the level of nonlinearity to the level of vibration response as a function of
273 both frequency and displacement level for the umbo (top graph) and the stapes (bottom
274 graph). Colour is used to represent the ratio, and the vibration response curves for sound
275 pressure levels of 108 dB, 114 dB and 120 dB have been added as solid black lines. The
276 ratio of nonlinearity to vibration response is only shown in zones where the level of
277 nonlinearity exceeds the noise level. When comparing both graphs we see that they closely
278 resemble each other, showing that the nonlinear behaviour at the level of the stapes is to
279 some extent the same as at the level of the umbo. At 120 dB SPL the vibration amplitude of
280 the umbo is around -15 dB (re 1 μm), and the nonlinearity levels are about 40 dB below the
281 response levels for frequencies between 125-1000 Hz. In the resonance peak at 1800 -
282 1900 Hz, the vibration response increases to -2 dB (re 1 μm). As a reference, we have
283 added a red dotted line of -15dB vibration amplitude in the graph. Along this line of constant
284 vibration level of -15 dB (re 1 μm) we see that the level of nonlinearities drops to -70 dB
285 below the vibration response.

286

287 **4. Discussion**

288 *Animal Model*

289 The availability of fresh human material is very limited, which induces the need to switch to
290 animal models in the development of a new measurement technique. The rabbit ear differs
291 significantly from the human ear, but they do share several features. The hearing range of
292 the common rabbit was determined by Heffner using behavioral audiometry (Heffner, 1980).
293 His experiments showed that at a sound pressure level of 60dB SPL the lower frequency
294 boundary of hearing in rabbit is 96Hz, and the upper boundary is 49kHz. This frequency
295 range partly overlaps with the human auditory range. The rabbit eardrum itself is thinner than
296 in humans (Buytaert et al. 2013), but the visco-elastic properties of the rabbit ear (Aernouts
297 et al. 2010), are in the same range as those measured in humans (De Greef et al. 2014).
298 Both human and rabbit ears do, of course, have three-ossicles with ligaments and tendons.

299 For interpretation of the current results, the most significant difference might be that in
300 humans the incudo-malleolar joint has been shown to be mobile at moderate sound pressure
301 levels (Willi et al. 2002) while in rabbits both ossicles are fused together (Soons et al. 2010),
302 allowing hardly any relative motion. So, in humans the motion in the articulation between the
303 incus and malleus may have an additional influence on the nonlinearities at the level of the
304 stapes.

305

306 *Influence of the Cochlea*

307 In our procedure we measured the motion of the footplate after removing the cochlea. This
308 approach allows us to measure perpendicular to the footplate, and also allows us to purely
309 test the middle ear system. The cochlea is known to possess highly nonlinear characteristics
310 due to its active feedback mechanisms, and it has been shown that the cochlea is able to
311 generate nonlinear distortions in the middle ear post mortem (Rhode 2007). Thus, removing
312 it eliminates the potential for these distortions, and we can be sure that what we measured
313 was entirely due to the middle ear system and not due to any remaining cochlear activity. A
314 further reason for choosing to remove the cochlea was due to the relative inaccessibility of
315 the stapes footplate in rabbits. In a preparatory experiment we measured vibration response
316 at the umbo before and after removal of the cochlea and we found only limited changes in
317 both vibration response and the level of the nonlinearities (Figure 2). The vibration response
318 remained practically unchanged for frequencies below 1 kHz but at higher frequencies some

319 changes were observed and vibration amplitudes slightly increased. The level of the
320 nonlinearities also remained largely unchanged, except at some of the lower frequencies
321 where some increase is seen. Overall the level of the nonlinearities did not change strongly,
322 but some effect of removal of the cochlea proved to be inevitable.

323

324 *Vibration Response*

325 At low frequencies the response curve is rather flat, gradually increasing to a resonance
326 peak, and for frequencies beyond this first resonance the curves become more complicated.
327 The vibration response at level of the stapes is largely a near-perfect copy of the vibration
328 response of the umbo, only 10 dB lower. In Figure 5 we see that the ratio is very constant up
329 to frequencies of 4 kHz, but at the highest frequencies the ratio of both responses somewhat
330 drops from 10 dB at 4 kHz to 0 dB at 16 kHz. Here we should emphasize that we were only
331 able to measure along one direction, and did not measure the full three dimensional motion
332 of the ossicles. It has been shown that at low frequencies the stapes performs a piston-like
333 motion (Huber et al. 2001; Hato et al. 2003) but that at high frequencies the motions become
334 much more complicated. It is therefore possible that in the 8-16 kHz octave our single-
335 direction measurement underestimates the maximal amplitude of stapes motion.

336 In Figure 8 we have shown the ratio of umbo vibration response to stapes vibration response
337 as a function of input sound pressure level. We have already described how the ratio of
338 umbo to stapes vibration response is practically constant, and we now see that the ratio of
339 nonlinear response also shows very little dependence on sound pressure level. At the lower
340 pressure levels the ratio is a little bit less than the ratio of the vibration response, and there is
341 a slight tendency for the ratio to increase at higher pressure levels. This means that at the at
342 the highest sound pressure levels the vibrations at the footplate show a bit less nonlinearity
343 than the vibrations at the umbo. If the sound transmission from malleus to stapes would not
344 have any influence on the non-linearities, we would expect the ratio to be equal to the ratio
345 of the vibration amplitudes. Apparently transmission of the sound along the ossicular chain
346 has some effect on the level of non-linearities, but the effect is marginal. At this instance we
347 do not have an explanation for the fact that at higher sound pressure levels the stapes
348 vibration response is a bit less non-linear than umbo vibrations response. In any case the
349 results show that the joints between the ossicles do not increase the non-linearities in the
350 vibration signal going to the cochlea.

351

352 *Nonlinearities as a function of frequency*

353 From Figure 5C we see that the curves showing the level of nonlinearities for umbo and
354 stapes resemble the curves of vibration response of both ossicles, but that there are also
355 important differences. Before the first resonance peak the curves are rather flat, just like the
356 vibration response curves. However, at the location of the first resonance (1800 - 1900 Hz)
357 the nonlinearity curves stay flat and do not show the same characteristic maximum. Beyond
358 the first resonance, the level of the nonlinearities shows a stronger decrease as a function of
359 frequency than the vibration response. We will come back to this observation when
360 discussing the 3D colour representation of the data.

361 In Figure 6 we have shown the ratio of the nonlinearities between the umbo and the stapes.
362 The gap between the nonlinearity curves is rather constant over the entire frequency range,
363 although the variability between data points is much larger than for the vibration response.
364 The ratio of nonlinearities remains largely between 5 and 15 dB. Here we should remember
365 that the levels of the nonlinearities are 40 dB to 70 dB lower than the levels of the vibration
366 amplitudes (see Figure 5), making the data much more noise sensitive. On the whole
367 however we see that the ratio between umbo and stapes vibration response and the ratio
368 between umbo and stapes nonlinearity as function of frequency show good resemblance.
369 We conclude that no significant nonlinearities are added to the vibration response when
370 vibrations are passed on from the umbo to the stapes.

371

372 *Nonlinearities as a function of sound pressure level*

373 In Figure 7 we showed how the vibration amplitudes and the level of nonlinearities increase
374 as a function of input sound pressure level. With our detection method, nonlinearities
375 become detectable at vibration amplitudes as low as -110 dB (re 1 μm) in the 1-2 kHz and 4-
376 8 kHz octaves. In the 250-500 Hz octave detectability is a bit less (about -90dB re 1 μm).
377 The reason is that laser vibrometry is a velocity sensitive technique, so measuring sensitivity
378 increases as a function of frequency. We have also seen that nonlinearities at the umbo can
379 be detected at sound pressure levels of 6 dB to 10 dB lower than for the stapes. It is
380 important to realise that these findings do not mean that nonlinearities are absent at lower
381 sound pressure levels, it only means that our method is not able to detect them at this point.
382 So, the nonlinearity detected at the umbo at 93 dB is probably also reflected at the level of
383 the stapes, but the nonlinear behaviour of the stapes remains below the detection level of
384 the current method. Since the vibration level at the umbo is about 10 dB higher than at the
385 stapes, it seems logical that more sound pressure is needed for stapes nonlinearity to

386 become detectable. This observation also emphasises the fact the level at which the
387 nonlinearities become detectable is of little interest in itself.

388 More important therefore is the way the nonlinearity levels change as function of input sound
389 pressure. When we compare the nonlinearity curves to the vibration response curves, we
390 clearly see that the level of nonlinearities increases more strongly as a function of sound
391 pressure level than the vibration response. When we make a linear fit to the output response
392 data as function of input sound pressure level, we find the gradient of the line to be
393 practically equal to one across all frequency bands. However, when we make a linear fit for
394 the nonlinearity data, we find the gradient to range from 1.7 to 2 in different frequency bands.

395 In Figure 8 we have shown the ratio of umbo nonlinearity to stapes nonlinearity as a function
396 of sound pressure level. We have already described how the ratio of umbo to stapes
397 vibration response is practically constant, and we now see that the ratio of nonlinear
398 response also shows very little dependence on sound pressure level. There is apparent a
399 slight tendency for the ratio to increase at higher pressure levels, meaning that at the highest
400 sound pressure levels the vibrations at the footplate show a bit less nonlinearity than the
401 vibrations at the umbo. At this instance we do not have an explanation for this observation,
402 and the effect is rather marginal. But some increasing “linearisation” of the vibration signal is
403 observed.

404

405 *Nonlinearity as function of frequency at constant vibration level*

406 We already mentioned above that the curves of nonlinearity as a function of frequency do
407 not show a peak in the frequency range corresponding to the resonance peak observed in
408 the vibration response curve. This observation is emphasized when looking at lines of
409 constant vibration amplitude in Figure 9. When we look at a vibration amplitude of -15 dB (re
410 μm) in the plot for the umbo, we see that this vibration response is reached at 120 dB SPL
411 for a frequency range between 125 Hz and 500 Hz. At frequencies going up to the
412 resonance peak the same vibration level is reached at lower sound pressure levels. When
413 looking at the nonlinearities however we see that in the region 125-500 Hz the level of umbo
414 nonlinear response is about 40 dB below vibration response, while at the resonance peak
415 the nonlinearities are more than 70 dB below vibration response. We find this a most
416 peculiar observation: apparently it is not (only) the amplitude of the motion which determines
417 the magnitude of the nonlinearity, as the same motion amplitude at one frequency results on
418 30 dB more nonlinearity as the same vibration amplitude at another frequency. In general we

419 see that, for the same vibration level, the nonlinearities are much more prominent at low
420 frequencies than at high frequencies.

421

422 *Source of the nonlinearities.*

423 Pinpointing the sources of the nonlinear responses we measured is beyond the scope of the
424 current paper, and will need a detailed modelling approach which we are planning for future
425 work. Possible sources of the nonlinear response are the nonlinear elastic properties and
426 damping properties of the eardrum and the ligaments, and the asymmetrical shape of the
427 eardrum. In quasi-static studies it has been shown that umbo displacement as a function of
428 pressure shows hysteresis (Dirckx et al. 2006) and is also asymmetric, which obviously
429 causes a nonlinear response, and it has been suggested that the tent-like shape of the
430 eardrum may play an important role in this observation. For the quasi-static pressure range
431 at large amplitudes (2 kPa), modelling has shown that the asymmetrical shape of the
432 eardrum is a crucial factor (Ladak et al. 2006). In the acoustic range displacements are far
433 smaller, but still the asymmetrical shape of the membrane may influence manubrium motion.
434 It is our current hypothesis that membrane geometry asymmetry is the major cause of
435 middle ear nonlinear response, and we will investigate this further both through modelling
436 approach and measurements in species with flat eardrums. From the current measurements
437 we see that the nonlinearities observed at the stapes are largely identical to the
438 nonlinearities seen at the umbo. This leads us to believe that the eardrum is the governing
439 component in the nonlinear response of the middle ear, and it certainly shows that no
440 significant additional nonlinearities are added to the vibration signal on its way through the
441 middle ear.

442

443 **5. Summary and Conclusion**

444 In this paper we measured the vibration response and the nonlinearities in the vibration
445 response of the umbo and the stapes. Using a very sensitive measurement technique we
446 were able to detect nonlinearities at input sound pressure levels of 93 dB SPL. In general,
447 we found that nonlinearities as function of frequency and as function of sound pressure
448 largely show the same behaviour for both the umbo and the stapes. Further research will be
449 needed to pinpoint the source of these nonlinearities, but the current results show that no
450 significant additional nonlinearity is generated as the vibration signal is passed through the
451 middle ear chain. As we do not see major differences between the nonlinear response

452 measured at the stapes and that measured at the umbo, the current results suggest that
453 measurements at the level of the eardrum are sufficient to detect middle ear nonlinearity.

454 Nonlinearities are most prominent in the lower frequencies (125 Hz to 1 kHz), where their
455 level is about 40 dB below vibration response at an input of 120 dB SPL. At lower sound
456 pressure levels nonlinearities are less prominent but we have demonstrated their presence,
457 and correct quantification of the effect may be relevant in the interpretation of nonlinear
458 cochlear responses measured through oto-acoustic emissions at higher sound pressure
459 levels. We also found that nonlinearities increase nearly twice as fast as the vibration
460 response when sound pressure levels increased. This indicates that middle ear nonlinear
461 distortions may become important when developing high power hearing aids which generate
462 sound pressure levels as high as 140 dB.

463

464 **Acknowledgements**

465 The authors wish to thank Fred Wiese and William Deblauwe for their assistance with the
466 measurement setup.

467 This work was supported by the Research Foundation Flanders - Fonds Wetenschappelijk
468 Onderzoek (FWO).

469

470 **References**

471 Aernouts J, Soons J, Dirckx JJJ (2010) Quantification of tympanic membrane elasticity
472 parameters from in situ point indentation measurements: validation and preliminary
473 study. *Hear Res* 263:177–82. doi: 10.1016/j.heares.2009.09.007

474 Aerts JRM, Dirckx JJJ (2010) Nonlinearity in eardrum vibration as a function of frequency
475 and sound pressure. *Hear Res* 263:26–32. doi: 10.1016/j.heares.2009.12.022

476 Buytaert J, Jeught S Van Der, Ars B, et al. (2013) Preliminary Human Tympanic Membrane
477 Thickness Data from Optical Coherence Tomography. In: Buytaert J, Dirckx J (eds)
478 *Opt. Meas. Tech. Syst. Struct. 2*. Shaker Publishing, pp 75–84

479 De Greef D, Aernouts J, Aerts J, et al. (2014) Viscoelastic properties of the human tympanic
480 membrane studied with stroboscopic holography and finite element modeling. *Hear Res*
481 312:69–80. doi: 10.1016/j.heares.2014.03.002

482 Dirckx JJ, Decraemer WF (2001) Effect of middle ear components on eardrum quasi-static
483 deformation. *Hear Res* 157:124–37.

484 Dirckx JJJ, Buytaert JAN, Decraemer WF (2006) Quasi-static transfer function of the rabbit
485 middle ear' measured with a heterodyne interferometer with high-resolution position
486 decoder. *J Assoc Res Otolaryngol* 7:339–51. doi: 10.1007/s10162-006-0048-5

487 Funnell WRJ, Heng Siah T, McKee MD, et al. (2005) On the coupling between the incus and
488 the stapes in the cat. *J Assoc Res Otolaryngol* 6:9–18. doi: 10.1007/s10162-004-5016-
489 3

490 Funnell WRJ, Khanna SM, Decraemer WF (1992) On the degree of rigidity of the manubrium
491 in a finite element model of the cat eardrum. *J Acoust Soc Am* 91:2082 – 2090.

492 Goode R, Killion M, Nakamura K, Ishihara S (1994) New knowledge about the function of the
493 human middle ear: development of an improved analog model. *Am J Otol* 15:145 – 154.

494 Guinan J, Peake W (1967) Middle -ear characteristics of anesthetised cats. *J Acoust Soc*
495 *America* 41:1237 – 1261.

496 Hato N, Stenfelt S, Goode R (2003) Three-dimensional stapes footplate motion in human
497 temporal bones. *Audiol Neurootology* 8:140–152.

498 Huber A, Linder T, Ferrazzini M, et al. (2001) Intraoperative assessment of stapes
499 movement. *Ann Otol Rhinol Laryngol* 110:31–5.

500 Ladak HM, Funnell WRJ, Decraemer WF, Dirckx JJJ (2006) A geometrically nonlinear finite-
501 element model of the cat eardrum. *J Acoust Soc Am* 119:2859. doi: 10.1121/1.2188370

502 Nedzelnitsky V (1980) Sound pressures in the basal turn of the cat cochlea. *J Acoust Soc*
503 *Am* 68:1676 – 1689.

504 Rhode W (2007) Distortion product otoacoustic emissions and basilar membrane vibration in
505 the 6 - 9 kHz region of sensitive chinchilla cochlea. *J Acoust Soc Am* 122:2725 – 2737.

506 Schoukens J, Lataire J, Pintelon R, et al. (2009) Robustness issues of the equivalent linear
507 representation of a nonlinear system. *IEEE Trans Instrum Meas* 58:1737–1745.

508 Soons J a M, Aernouts J, Dirckx JJJ (2010) Elasticity modulus of rabbit middle ear ossicles
509 determined by a novel micro-indentation technique. *Hear Res* 263:33–7. doi:
510 10.1016/j.heares.2009.10.001

511 Voss S, Rosowski J, Merchant S, Peake W (2000) Acoustic responses of the human middle
512 ear. *Hear Res* 150:43–69.

513 Willi UB, Ferrazzini M a, Huber AM (2002) The incudo-malleolar joint and sound
514 transmission losses. *Hear Res* 174:32–44.

515

516

517 **Figure Captions**

518 **Fig. 1** (A) photograph of the prepared specimen with the measurement points indicated, (B)
519 a 3-D rendering of the ossicular chain obtained from a CT scan. In (B) the direction of the
520 laser beams is indicated by the red dashed line, in (A) the laser beam direction is
521 perpendicular to the plane of the photograph. In figure 1B the tympanic membrane is
522 coloured red, the malleus blue, the incus green, and the stapes purple.

523 **Fig.2** Vibration response (squares) and amplitude of non-linearities (triangles) measured at
524 the umbo before (blue) and after (red) removing the cochlea. This data was obtained at a
525 sound pressure level of 117 dB.

526 **Fig. 3** Vibration amplitude measured in five individual ears as a function of frequency; (A):
527 umbo, (B): stapes; (C) ratio of umbo to stapes vibration amplitude

528 **Fig. 4** Amplitude of non linearities measured in five individual ears as a function of
529 frequency; (A): umbo, (B): stapes; (C) ratio of umbo to stapes non-linearity amplitude

530 **Fig. 5** Vibration response and non-linearities amplitude for umbo and stapes as a function of
531 frequency. Data is averaged over five ears, and standard deviations are added;
532 measurements made at (A) 90 dB SPL, (B) 108 dB SPL, (C) 120 dB SPL.

533 **Fig. 6** Ratio of umbo to stapes vibration amplitude (diamonds) and nonlinearity amplitude
534 (squares) as a function of frequency at 117dB SPL sound pressure level. Data is averaged
535 over five ears, and standard deviations are added.

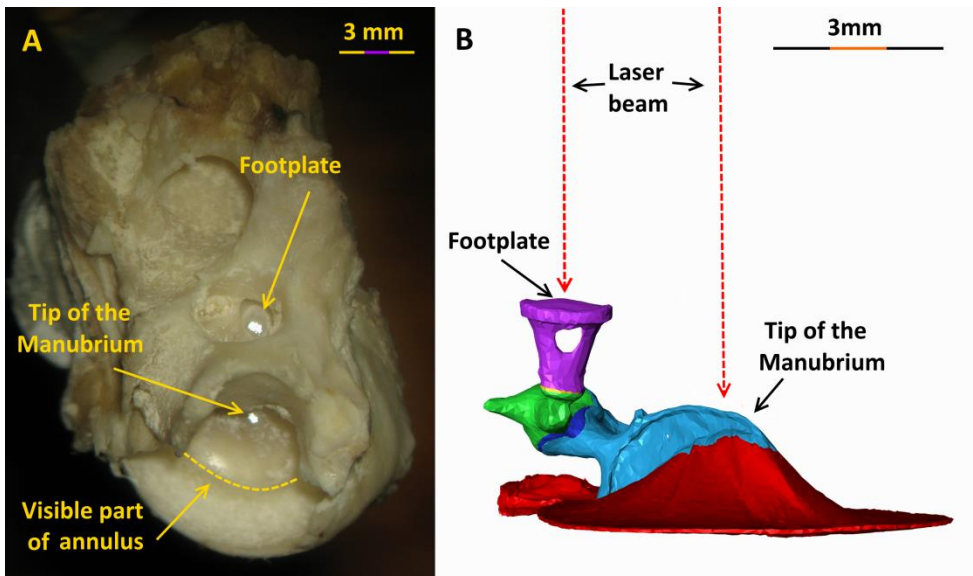
536 **Fig. 7** Vibration response and non-linearities amplitude for umbo and stapes as a function of
537 sound pressure level. Data is averaged over five ears, and standard deviations are added;
538 data obtained in frequency band (A) 125Hz to 500 Hz, (B) 1kHz to 2kHz, (C) 4kHz to 8kHz.

539 **Fig. 8** Ratio of umbo to stapes vibration amplitude (diamonds) and nonlinearity amplitude
540 (squares) as a function of sound pressure level. Data is averaged over five ears, and
541 standard deviations are added. Data obtained in the frequency bands (A) 125Hz to 500 Hz,
542 (B) 1kHz to 2kHz, (C) 4kHz to 8kHz.

543 **Fig. 9** Vibration amplitude and ratio of non-linear distortion to vibration response as a
544 function of frequency. Top graph: umbo; bottom graph: stapes. Dotted lines indicate vibration
545 responses at 180 dB, 114 dB and 120 dB sound pressure level. Ratio of distortions to
546 vibration response is indicated in colour. The horizontal line is added as a reference to see
547 how the ratio changes as function of frequency for fixed level of vibration amplitude.

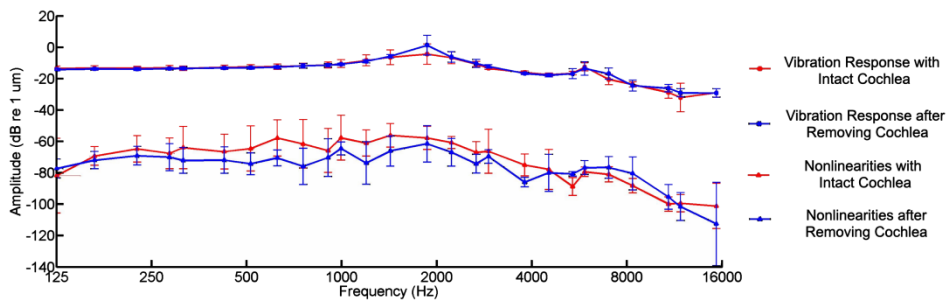
548

549 **Figure 1**



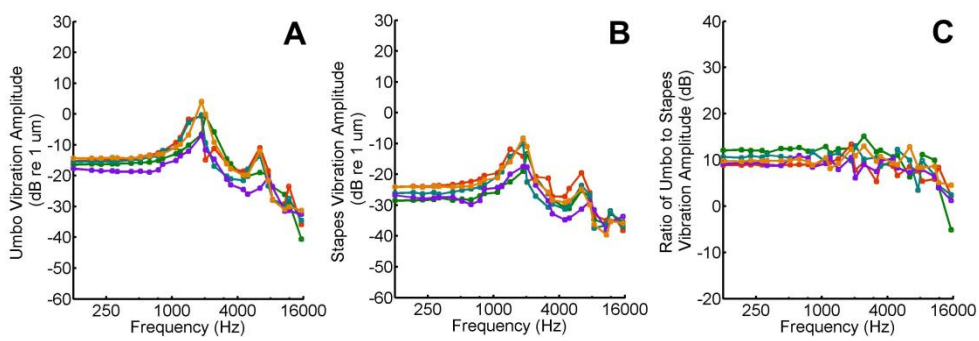
550

551 **Figure 2**



552

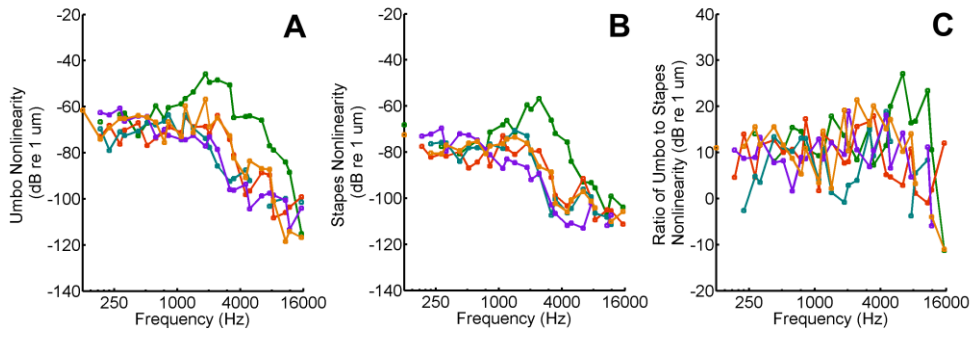
553 **Figure 3**



554

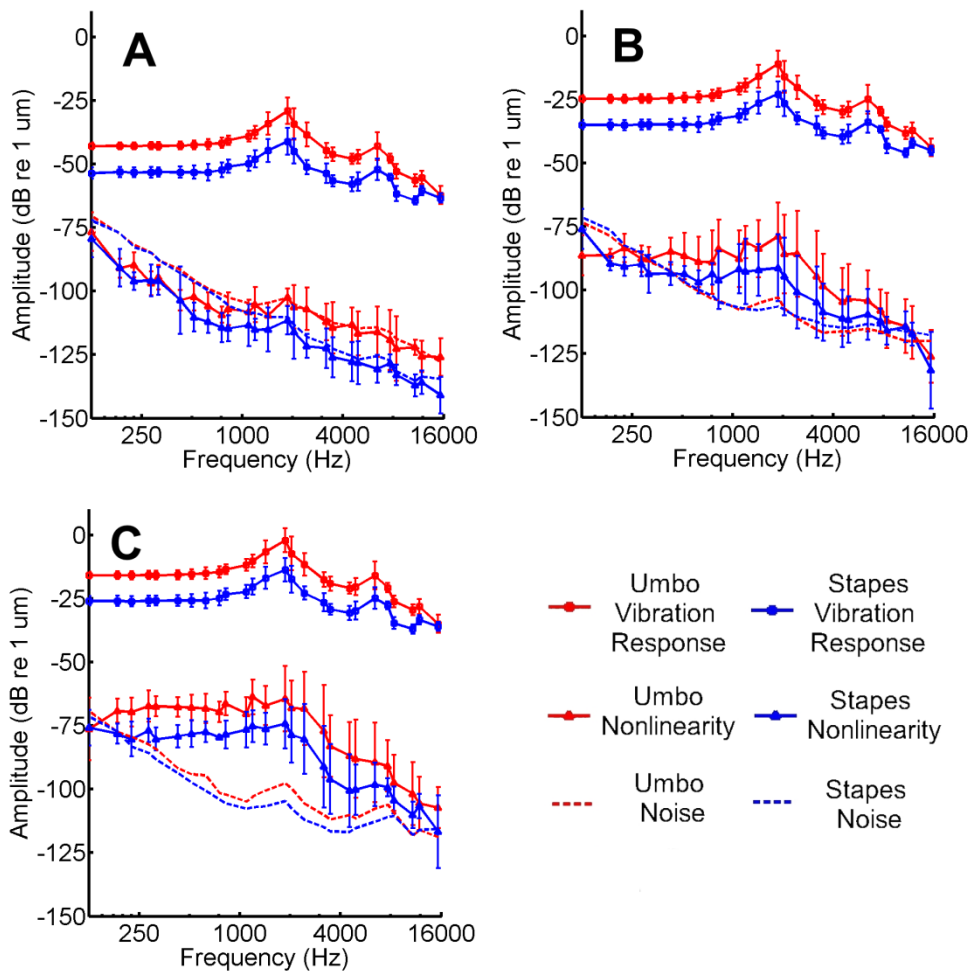
555

556 **Figure 4**



557

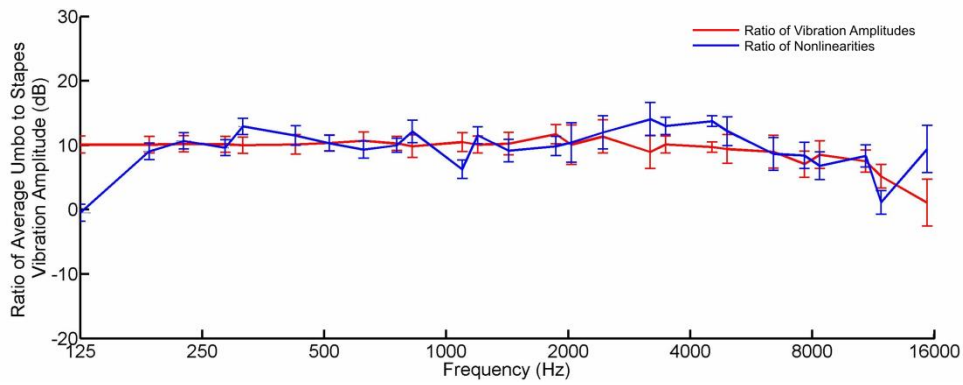
558 **Figure 5**



559

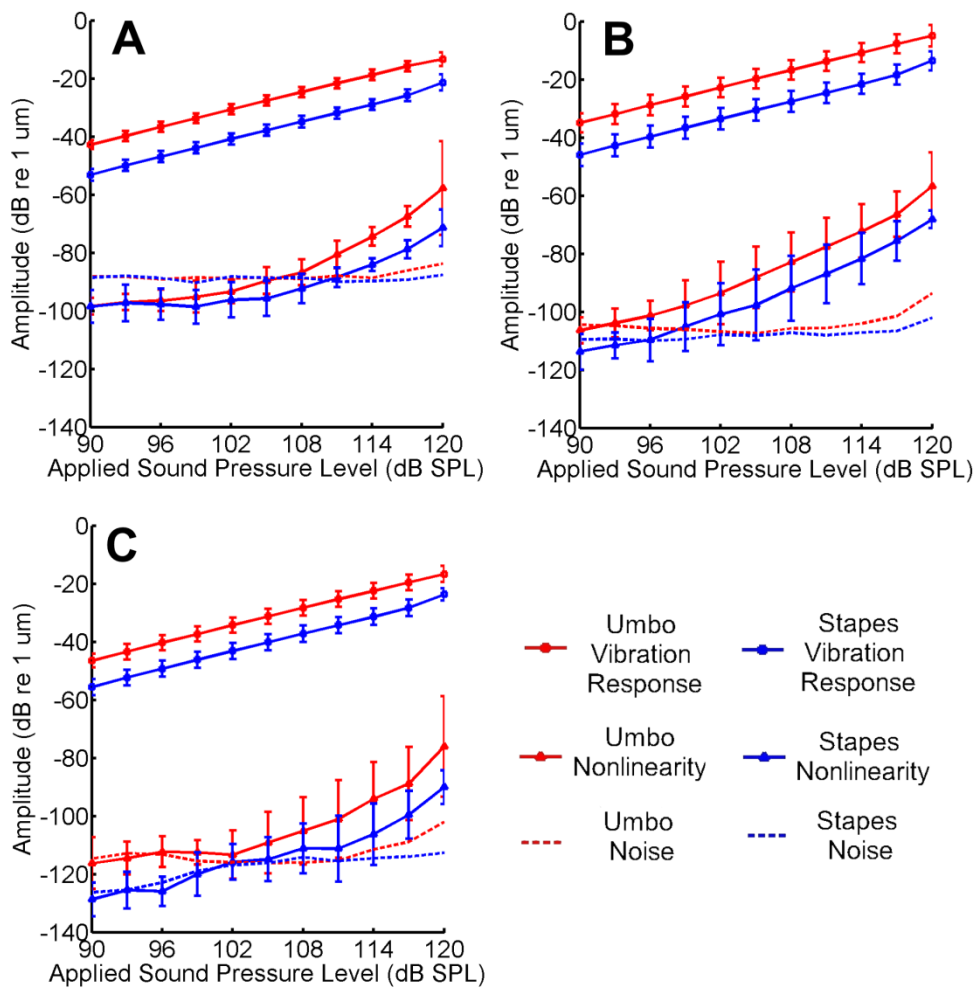
560

561 **Figure 6**



562

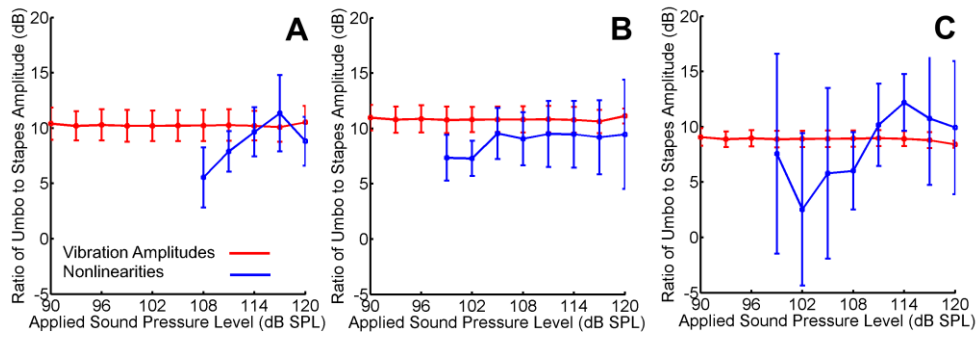
563 **Figure 7**



564

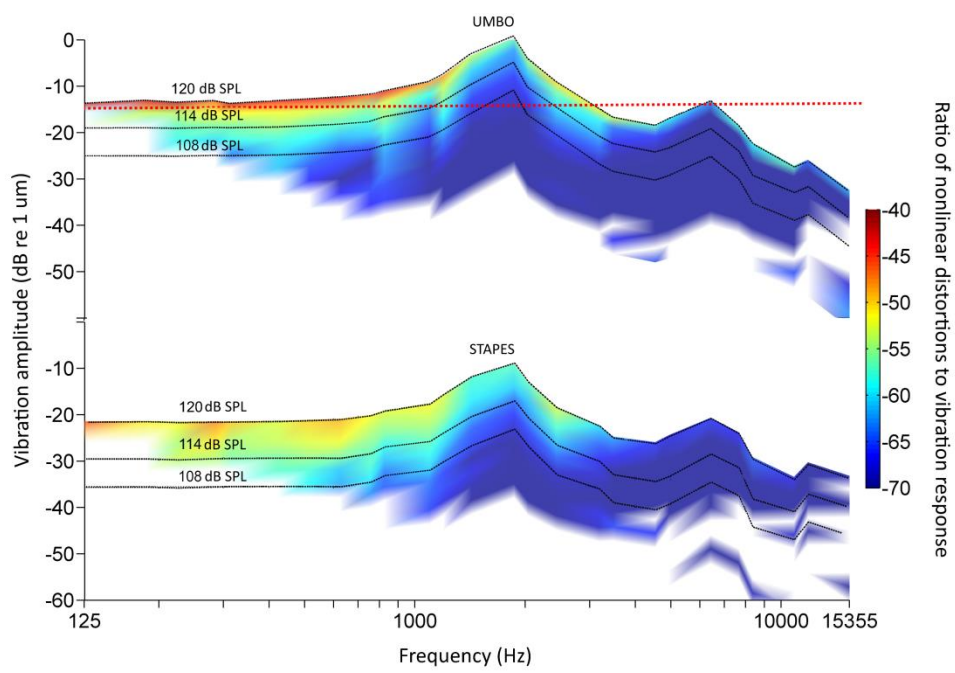
565

566 **Figure 8**



567

568 **Figure 9**



569

570

571

572